Renewable Energy Research Center

Progress toward 22% efficient n-type bifacial solar cell by applying boron emitter selectively doped structure

○Shalamujiang Simayi, Toshimitsu Mochizuki, Yasuhiro Kida, Katsuhiko Shirasawa, Hidetaka Takato

Photovoltaic Power Team, Renewable Energy Research Center, AIST

Research Background

Background [i]

- Bifacial solar cell is one of the main concept which increases the cell efficiency and decreases the cell cost.

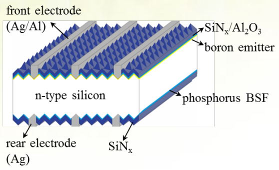

Figure 1: N-type bifacial solar cell structure.

n-type bifacial cell fabrication process

1. Saw damage removal
2. Texturization and RCA cleaning
3. BBr_3 diffusion (tube furnace)
4. Rear side boron doped layer removal
5. $POCl_3$ diffusion
6. BSG and PSG removal
7. Passivation layer
8. Electrodes screen printing
9. Firing
10. Edge isolation

Table 1: N-type bifacial solar cell I-V result.

Incident	J_{sc} [mA/cm²]	V_{oc} [mV]	FF [%]	η [%]
p^+ side	39.2	643.6	80.5	20.3
n^+ side	36.2	642.2	80.6	18.7

Evaluate the both sides passivation quality: IQE mapping for front and rear surfaces of 20% efficient bifacial solar cell.

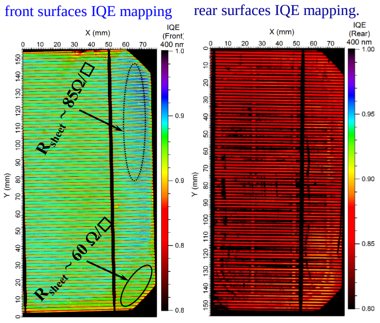

Figure 2: IQE mapping of the bifacial solar cell.

J_{0e} mapping of p^+np^+ symmetric lifetime sample passivated by SiN_x/Al_2O_3 stack.

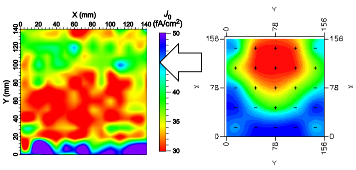

Figure 3: J_{0e} mapping boron emitter.

- Correlation of J_{0e} and IQE mapping was observed.
- Non-uniformity of boron emitter sheet resistance effects to the cell uniformity.

Background [ii]

Best PC1D fit to the experimental IQE data of 20.03% efficient bifacial solar cell.

Table 2: PC1D fitting parameters.

Device area	239 cm²
Front surface	Texture
Rear surface	Texture
Front reflectance	sample
Wafer thickness	180 µm
Wafer background doping	2.6×10^{15} cm^{-3}
Boron peak concentration	4.5×10^{19} cm^{-3}
Boron sheet resistance	70 Ω/□
Depth factor	0.22 µm
Bulk lifetime	600 µs
Series resistivity	2.5 mΩ
Fill factor	80.2%

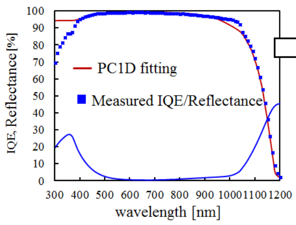

Figure 4: PC1D fit to the IQE of the cell.

Table 3: PC1D fit to the IQE of the cell.

	PC1D fit data	Measured data
Bulk lifetime [µs]	600	600
J_{sc} [mA/cm²]	38.8	38.7
V_{oc} [mV]	645.3	645.4
Fill factor [%]	80.2	80.2
FSRV** [cm/s]	2700	
RSRV** [cm/s]	5000	

Implies: High recombination at the front and rear sides of the cell.

Purpose of the Research

To reduce the front side recombination losses, a cell structure as shown in figure is necessary in which front side boron selective emitter with heavier and deeper boron doping profile underneath front contact metal. In this study, we focus on the boron emitter etch-back process, its recombination analysis, and estimation of cell performance potential by PC1D simulation.

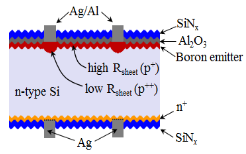

Figure 5: Selective boron emitter bifacial solar cell structure.

Experimental Method

Experiment [i]: etched back boron emitter

Etch-back boron emitter wafer process:

1. Mirror wafer by chemical etching
2. RCA cleaning
3. Baseline BBr_3 diffusion → R_{sheet} = 49 Ω/□
4. BSG removal
5. Boron emitter etch-back ← Chemical solution: HF/HNO_3 mixture

N-type CZ silicon	
Wafer size	156 × 156 mm²
Wafer thickness	180 µm
Wafer resistivity	~ 2.1 Ω cm
Bulk lifetime	~ 2 ms

Experiment [ii]: Passivation quality

symmetrical $p^+/n/p^+$ lifetime sample

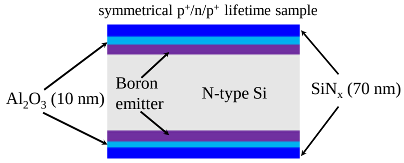

Lifetime was measured by quasi-steady-state micro-photoconductance decay (QSS-µPCD) measurements and QSS-PCD method.

Results and Discussion (i)

- **etched-back boron emitter sheet resistance and SIMS profile estimation**

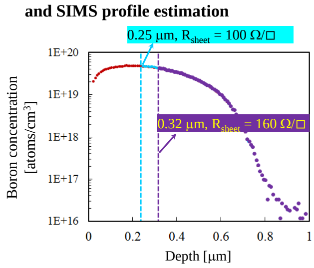

Figure 6: The estimated boron SIMS profiles.

Table 4: Corresponding boron sheet resistance and doping concentrations after etch-back process.

	Baseline boron	0.25 µm etched	0.32 µm etched
R_{sheet} [Ω/□]	49	100	160
Boron peak doping concentration [cm^{-3}]	4.8×10^{19}	4.3×10^{19}	4.0×10^{19}
Doping depth [µm]	0.85	0.6	0.53

- **Evaluation of passivation quality**

□ J_{0e} was extracted: $\frac{1}{\tau_{eff}} = \frac{1}{\tau_{bulk}} + \frac{2}{W}\frac{J_{0e}(N_A+\Delta n)}{qn_i^2}$

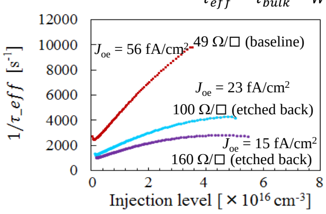

Figure 7: Inverse effective lifetime as a function of the injection level for J_{0e} samples.

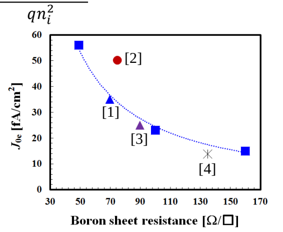

Figure 8: Comparison of J_{0e} with other research.

□ *Imp-Voc* of boron emitters.

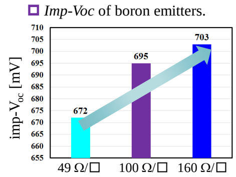

Figure 9: *Imp-Voc* of etched back boron emitter.

- **Discussions**

(i) Lifetime shows a linear behavior up to high injection level.
(ii) Saturation current density J_{0e} was improved significantly from 56 fA/cm² to 15 fA/cm² due to the lower recombination velocity while the sheet resistance increases to 160 Ω/□.
(iii) The comparison of J_{0e} values with various research results imply quite competitive passivation layer was applied on the boron emitter.

Results and Discussion (ii)

Performance analysis of bifacial solar cell by PC1D simulation

Table 5: PC1D fitting parameters based on the baseline cell.

Device area	239 cm²	
Front reflectance	sample	
Wafer thickness	180 µm	
Wafer background doping	2.6×10^{15} cm^{-3}	
Boron peak concentration	4.5×10^{19} cm^{-3}	
Boron sheet resistance	40 ~ 180 Ω/□	
Depth factor	0.15 ~ 0.6 µm	
Phosphorus peak concentration	6.0×10^{20} cm^{-3}	
Phosphorus peak concentration = 6×10^{19} cm^{-3}		
Bulk lifetime	600 µs	2000 µs
Series resistivity	2.5 mΩ	1 mΩ
Fill factor	80.2%	82%

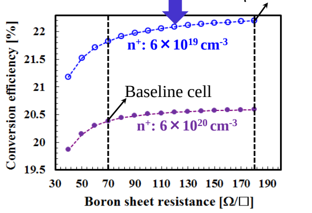

Figure 10: PC1D simulation for cell performance dependence of front side boron emitter and rear side doping concentration.

Conclusion

1. An important step was made to improve the front side emitter. Improved boron emitters were obtained by a chemical etch-back boron emitter process.
2. The J_{0e} was improved from 56 fA/cm² to 23 fA/cm² and 15 fA/cm² by increasing the boron sheet resistance to 100 Ω/□ and 160 Ω/□ respectively. V_{oc} improvement was expected due to the improvement of J_{0e}.
3. A n-type bifacial solar cell performance was analyzed by PC1D simulation.
4. A large gain was expected by reducing the rear side doping concentration.

R_{sheet} = 160 Ω/□, n+: 6×10^{19} cm^{-3} → J_{sc} = 0.0395 A/cm², V_{oc} = 685.5 mV, FF = 82 %

References

[1] S. Simayi *et al.*, 77th Japan Society of Applied Physics Autumn Meeting, 2016.
[2] A. Richter *et al.*, Proc. 27th European Photovoltaic Solar Energy Conference and Exhibition, pp. 1133 – 1137 (2012).
[3] A. Richter *et al.*, Proc. 25th European Photovoltaic Solar Energy Conference and Exhibition, pp. 1453 - 1459 (2010).
[4] J. Benick *et al.*, Proc. 24th European Photovoltaic Solar Energy Conference and Exhibition, pp. 863 – 870 (2009).